The Formula One Tire Changing Robot (F1-T.C.R.)

RAUL MIHALI and TAREK SOBH
Department of Computer Science and Engineering
University of Bridgeport, Bridgeport, CT 06601

Abstract:

Formula One racing is one of the most fascinating sports ever, a perfect combination of high speed, technology, pressure and danger.
One problem associated with car racing is the time difference between teams during pit stops, which basically affects substantially the final results. In addition, a high percentage of the accidents in Formula One is due to pit stop problems. Changing the tires of a car while almost in motion, after reaching dangerous pressure and temperature values, is a very risky challenge, no matter how well a team is trained. Approximately 15-25 people are constantly exposed to serious dangers. Even though these stops might be a great fun for fans, the risks taken are extreme and any idea of reducing it without affecting the quality of the race should be considered. In the example from Figure 1, due to the malfunctioning of the refueling equipment, the entire team including the pilot had to risk their lives.
Our idea is to build a fully robotized system that takes over the tire changing process and also refueling, practically no need for human intervention. The system should demonstrate remarkable time accuracy, precision and low risk implications. This paper will detail the process and the bases of the system. Refueling is not being discussed here, however, the approach is very similar with the tire changing arms.

1. GENERAL CONSIDERATIONS

In order to maintain the quality of the race, the first parameter to be optimized is the *time accuracy*. More specifically, the robot has to change the tires of any car within the same time quantum. The current variance of *seconds* achieved by pit stop teams requires remarkable experience, but does not prove sufficient in a race. A precision of 0.1 seconds or better is required. In the first version of our proposed system, a process length of 10 to 15 seconds will be achieved, and will be optimized to 6-8 seconds later. A visual system will be implemented too. Another constraint is the *environment's limitations*. Only moderate changes in the pit stop's configuration can be allowed, due to the severe FIA regulations.

Fig. 1. Pit accident (Benneton team, 1994, Germany).

2. BRIEF MECHANICAL APPROACH

2.1. Considerations / Arms / Workspace

Our proposed robotic system consists of 5 manipulators: one for each of the tires, and a fifth one for the fuel tank. To preserve the environment of the pit stop and to assure the comfort of the team we implement suspended manipulators. The support of the 5 arms (Figure 2) allows the sliding motion of each arm and also does not create any obstacles or driving difficulties for the pilot.

Fig. 2. View from the track side

The support has 2 double longitudinal branches on which the arms are to be suspended, 2 arms on one pair of branches, and 3 on the other one. The sliding mechanism of the arms is essential for the end effector positioning. The material has to be resistant, of low elasticity and capable of sustaining the mass of the arms. An aluminum derivative can be used.
Each of the tires of a Formula One car is fixed to the body with a single central screw (Figure 3). This design allows a much flexible end - effector with less required power and mass, however, a multi-screw design is pending too.

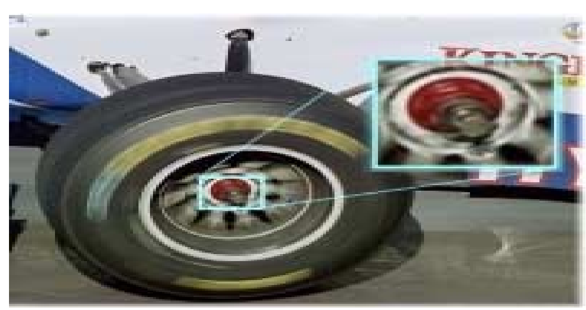

Fig. 3. Tire close-up

Each of the manipulators has a sliding range of 1 to 1.5 meters on the supports and can handle a tire in many ways. The only plane in which a good dexterousity is required is the horizontal one, due to the fact that the distance from the ground and the tire's central axis is relatively constant. Based on the abovementioned requirements, the manipulator design from Figure 4 has been reached.

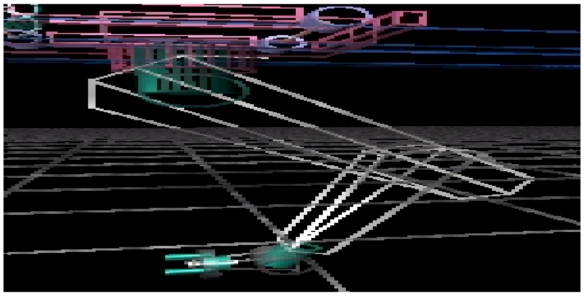

Fig. 4. Wire-frame side view

2.2. Tasks And Motion Related Briefings

The car arrives into the pits from a certain direction and stops in approximately the same position every time. By the time the car arrives, the visual system registers it and notes the exact position and direction of the tires. Once the car stops and is jacked up, the arms can start the *tire changing process*. For lifting the car, a simple lifting system will be positioned on the stopping platform. The problem is easily solvable and not discussed further in this paper. Each tire handling manipulator has to go through the following task sequence:

- Position the end effector as a function of the tire parameters received from the visual system
- Rotate the end effector so that it can catch the tire
- Grab the tire
- Remove the screw
- Remove the tire from its axis and put it on the ground near the car in a convenient spot
- Change the position and grab a new tire, located in the proximity, with a new screw on it
- Reposition the end effector and mount the new tire
- Tighten the screw
- Move back in the *stand-by* position to enable the car's departure.

There are about 15 different moves to be done, each one in about 1 second, which would allow a process length of approximately 10-12 seconds per manipulator. Of course all the arms work in parallel and independently. The positioning of the end effector and actually the entire set of movements required are of short distance and mainly consist of revolute steps: arm expansion/contraction, arm/end effector rotation and end effector positioning. There is a good chance that the specified time of around 1 second per move can be reduced. Four sensors are being mounted on each tire, responsible for specifying the tire's angle and position relative to the arm. According to the information from these sensors, the end effector can position itself perpendicularly on the tire and grab it correctly. We did not have yet the chance to work on a real car, but the system can be easily adjusted to handle similar tires based on one screw. The sensors can also be bolt into the rims and they only have to be detectable by radar. The rotation of the screw is a simple task, implying the activation of one compressed air tool with good dynamics control.
The most time consuming event is handling of the tire itself. This task requires good torque and acceleration control on the entire arm, implying the activation of all the engines, including precision sliding. We estimate the time interval from removing the old tire and replacing it with the new one of being of 3 to 5 seconds. Moving back in the *stand-by* position is again a simple task, completed partially when the car leaves (as long as the arms are at a safe distance from the tires, the car can go). Because of the sliding mechanism, the pilot can allow errors of up to half a meter while parking. However, there are still some exceptional positions, which will require special attention.

2.3. Joint / Link Requirements And Construction

One arm is composed of 4 joints and the end effector. The first joint is prismatic and constitutes the sliding part of the system (Figure 5).

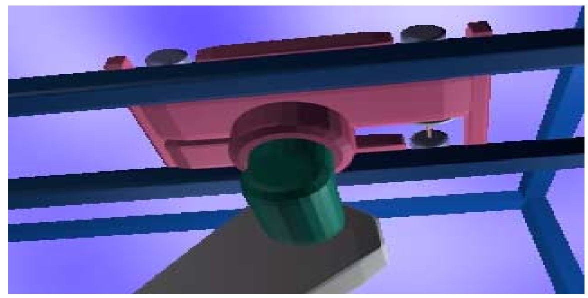

Fig. 5. The slider (beneath)

The prismatic movement is controlled by one engine fixed above the slider. The engine's torque/mass ratio doesn't have to be tight, and a sliding accuracy of 1mm is sufficient. Typically, the slider is activated just in the beginning of the full tire changing process, to fix the arm in an appropriate position. The friction coefficient of sliding between the support and the 4 wheels has be large enough to allow a stable braking with a precision of $1m/s^2$ and the friction coefficient of revolution has be small enough for low acceleration control. The joint has a braking mechanism (not visible in the figure) that activates once the requested position is achieved. This blocks the arm on the support while changing the tire, thus reducing the vertical and horizontal vibrations. All the engines work at high speeds and have significant mass, and so the inertia problem has to be considered thoroughly ([4, 6, 10]). Controlling this joint is the easiest task since it does not have to be part of the controlling equations (shown later in the paper). To optimize the time, the arm moves from / to the stand-by position to / from the ready position in the same time with the sliding action (more details in the *Controlling* related section).
The second joint is revolute, as all of the following ones. Figure 6 shows the joint and indicates the rotation direction.

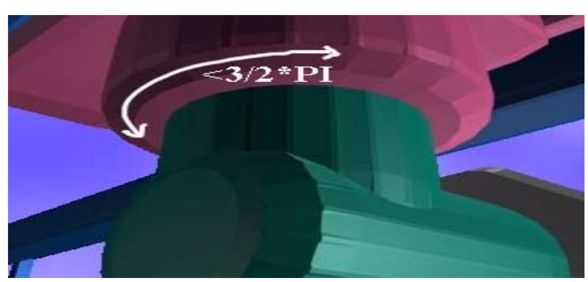

Fig. 6. Second joint (bottom left view - car side)

It is an essential orientation joint with a strong engine, supporting most of the tensions of the other engines. A revolution limitation of 3/2*PI is subjective, but it will avoid kinetic or dynamic problems (e.g. singularities). The engine is fixed in the sliding part (here red color), thus allowing flexibility in mass, most of the pressure being handled by the normals between the support and the 4 wheels.

The third joint is closely mounted near the previous one, and together with it and the sliding joint forms the *rigid* concentration of mass and torque of the arm (Figure 7).

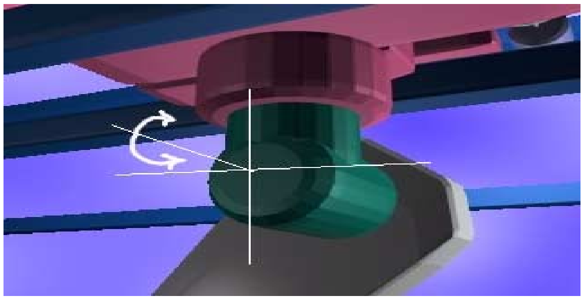

Fig. 7. Third joint (view from car side.)

In order to keep the torque high in this part of the arm and a good torque control in the next joints, the engine of this joint has been attached to the axis of the previous joint. The rest of the arm has to be as light as possible as it forms the *transportable* part. The angle of rotation has been limited to less than PI/2 degrees.

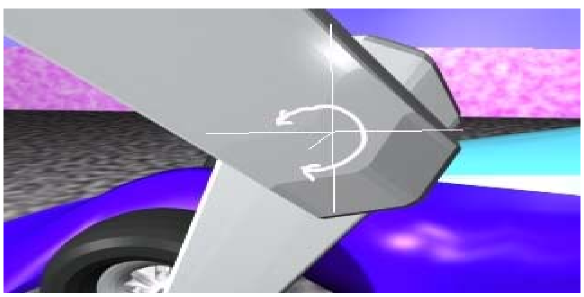

Fig. 8. Elbow joint

The last revolute joint from the arm segment is the elbow joint (Figure 8). This joint's engine has a moderated torque and is light. The transportable part of the arm has to be as light weighted as possible in order to achieving the required speed. It is installed in the upper part of the arm, thus keeping a safe distribution of mass. The angle of revolution has been limited to PI/2 degrees (avoids singularities and fits the requested tasks). By adjusting the mass of this engine, this part of the arm will check the balance for the entire system. The pressure should be as small as possible on the contacts between the support and the arms, especially while the 5 arms work together and the vibrations in the support are high, forcing dislocation. The critical positions of the arm are the *stand-by* one and the *fully extended* one (Figures 9 and 10).

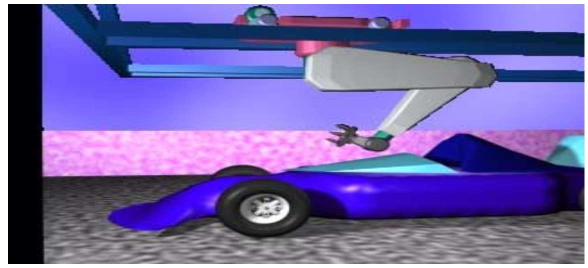

Fig. 9. *Stand-by* position

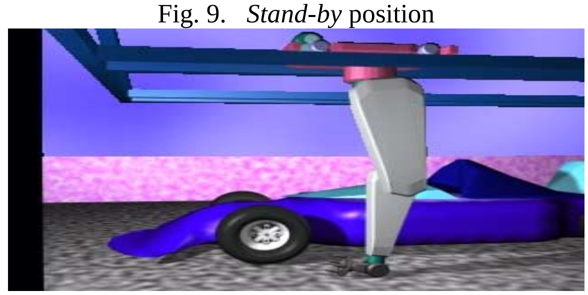

Fig. 10. *Fully extended* position

The fully-extended position (at about PI for the third joint and PI/2 for the fourth joint) would already require special orientation for the end effector, otherwise touching the ground. The stand-by position is safe enough to offer the pilot a good visibility while entering the pits. As an example the car does not exceed 1m in height and the slider of the arm is situated at about 2m above the ground.

2.4. The end effector (design / power / accuracy)

The end effector has to be small and light, but powerful, dexterous and quick. After various models, we came up with the design from Figure 11.

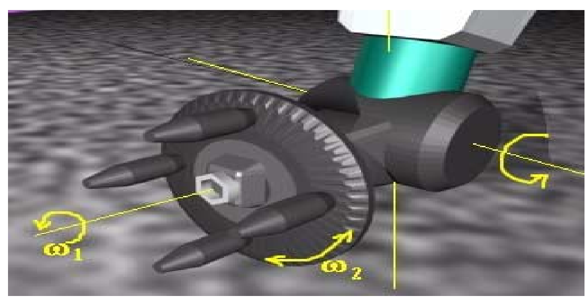

Fig. 11. End effector

This model solves all of the problems so far. First, there are no positioning problems. The disk type effector can rotate at a speed ω_2, and reach any orientation requested by the visual system. Having 4 identical segments, there are no equilibrium problems during transportation. The electromagnetic forces are well distributed and allow movements within a wide acceleration range.

The revolute joint between the arm and the effector allows a rotation in the vertical plane of PI/2 degrees. The engine is light with moderate torque requirement. It is installed in the cylinder in order to allow for uniform mass distribution in the entire arm. The engine that spins the disk with the 4 segments is installed in the pyramidal body following the cylinder, in the same spot with the compressed-air system for screw removal.

The only rotation that cannot be performed by this end effector is on the vertical axis. However, this rotation is achieved by the first revolute joint, which supports most of the torque requirements and allows for good acceleration control. In this setup, the end effector can operate for almost any reachable position of the tire. Another advantage of this effector model is that the tire does not have to be perpendicular to the ground (supposing an accident has happened). The end effector would still be able to accommodate the correct orientation. However, once the tire is not perpendicular to the ground this would mean that the car has been damaged seriously and most probably needs intervention of the team (another advantage of mounting sensors in the tires).

A small issue to be clarified is how the compressed air screwdriver finds the position of the screws: the screw driver starts a revolute task and at the same time tries to advance slowly until it "fits" the faces of the screw and fixes onto the screw.

3. DIRECT AND INVERSE KINEMATICS

One of the next steps is solving the direct and inverse kinematics for this specific manipulator (Figure 12).

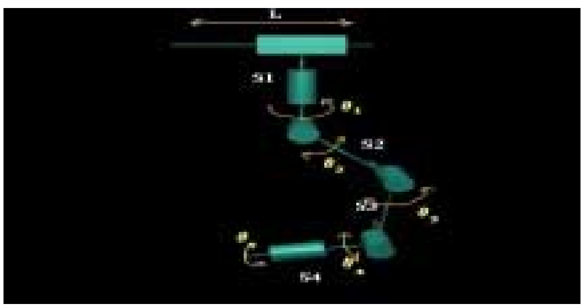

Fig. 12. Manipulator scheme A

Here, 6 joints of the arm can be seen. Using the Denavit-Hartemberg table [2], the equations for the direct kinematics can be written (the dimensions of the links are considered known):

$X = L + \cos(\theta_1) * (S2 * \sin(\theta_2) - S3 * \sin(\theta_2 + \theta_3) - S4 * \sin(\theta_2 + \theta_3 + \theta_4 - PI)$

$Y = -\sin(\theta_1) * (S2 * \sin(\theta_2) - S3 * \sin(\theta_2 + \theta_3) - S4 * \sin(\theta_2 + \theta_3 + \theta_4 - PI)$

$Z = S1 + S2 * \cos(\theta_2) - S3 * \cos(\theta_2 + \theta_3) - S4 * \mathrm{Cos}(\theta_2 + \theta_3 + \theta_4 - PI)$

$\theta_x = 0$

$\theta_y = 3 * PI/2 - (\theta_2 + \theta_3 + \theta_4)$

$\theta_z = \theta_1$

Where X, Y, Z, are the coordinates and θ_x, θ_y, θ_z the orientations of the end effector.

Solving for the inverse kinematics using direct algebraic methods [14], we obtain the following model:

$L = (Y / \tan(\theta_z))$

$\theta_1 = \theta_z$

$\theta_3 = \arccos((S2 * S2 + S3 * S3 - (X + S4 * \sin(PI/2 - \theta_y) * \cos(\theta_z) - (Y / \tan(\theta_z))) * (X + S4 * \sin(PI/2 - \theta_y) * \cos(\theta_z) - (Y / \tan(\theta_z))) - (Z + S4 * \cos(PI/2 - \theta_y) - S1) * (Z + S4 * \cos(PI/2 - \theta_y) - S1)) / (2 * S2 * S3))$

$\theta_2 = \arccos((-(S3 * \sin(\theta_3)) * ((X - (Y / \tan(\theta_z))) / \cos(\theta_1) + S4 * \sin(PI/2 - \theta_y)) + (S2 - S3 * \cos(\theta_3)) * sqr((S2 - S3 * \cos(\theta_3)) * (S2 - S3 * \cos(\theta_3)) + (S3 * \sin(\theta_3)) * (S3 * \sin(\theta_3)) - ((X - (Y / \tan(\theta_z))) / \cos(\theta_1) + S4 * \sin(PI/2 - \theta_y)) * ((X - (Y / \tan(\theta_z))) / \cos(\theta_1) + S4 * \sin(PI/2 - \theta_y)))) / ((S2 - S3 * \cos(\theta_3)) * (S2 - S3 * \cos(\theta_3)) + (S3 * \sin(\theta_3)) * (S3 * \sin(\theta_3))))$

$\theta_4 = 3 * PI/2 - \theta_y - \theta_2 - \theta_3$

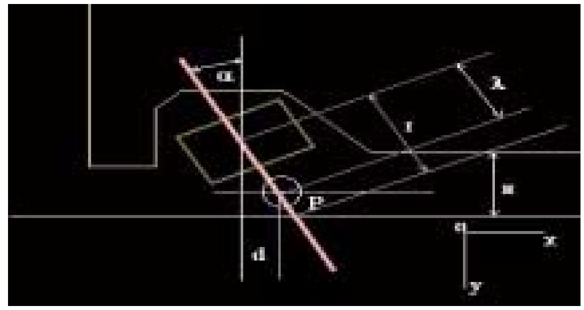

Fig. 13. Front left tire scheme (top).

The metrics referred is shown in Figure 14. The origin XYZO is at the left end of the slider and so we have a positive moving distance. The positions of the tire are referred by the visual system to the same XYZO.

For the first joint, the angle does not have to exceed PI degrees. As initial position (or stand-by), the angle will be always positioned at 0 degrees. The following 3 joints have been referred in terms of the previous link direction. For joint 2, the angle doesn't have to exceed PI/2. The angle will reach a value close to 0 degree very rarely (when the car is situated further away from the arm, about 80cm or more). The initial position of this angle will be set close to PI/2, so the link will go up.

For joint 3, the reference to the previous link proves a superfluous allowance for the angle, because the architecture of the robot does not allow angles less than PI/12. So we use values between PI/12 and up to PI. For the stand-by position the angle will be set around PI/12.

Joint 4 has lower limits than physically possible. The angle value will not be smaller than PI/4 and no bigger than 5*PI/4. Very small angles simply cannot be reached because of the architecture of the arm. Slightly larger angles (close to PI/4 or 5*PI/4) would cause problems holding the tire. A value of PI/2 is used for the stand-by position and also for the P position.

The final joint is adjusted independently from the others. The rotation direction matters as regards to controlling the torque. The value can run from 0 up to 2*PI. A software tracking system is being built, allowing rotating the 4 segments synchronously from the moment the visual system gives information about the tire's position. Thus, the angle can go up to n*PI. This is useful when the achieved speed is not satisfactory and there is a need to position the tools in advance.

For velocity and acceleration kinematics, the equations obtained from the D-H table define a function between the Cartesian space of positions and directions and the joint positions. We determine the velocity deriving the Jacobean of this function. Decoupling of singularities is not necessary as long as the design allows the avoidance of these. The inverse velocity and acceleration result from the following derivations:

$$dq = J(q)^{-1} * dX$$

$$d^2q = J(q)^{-1} * b$$

Where

$$B = d^2X - d/dt * J(q) * dq$$

$$d^2X = J(q) * d^2q + d/dt * J(q) * dq$$

Where:

$\boldsymbol{q}$ **=** the vector of joint coordinates;

$\boldsymbol{J(q)}, \boldsymbol{J(q)^{-1}}$ = the Jacobean and inverse Jacobean of $\boldsymbol{q}$

$\boldsymbol{X}$ = the vector of end effector coordinates

4. DIRECT AND INVERSE DYNAMICS

For this type of arm the following dynamics model ([1, 3, 4, 5]) is used:

$$\tau = M(q) * d^2q + V(q,dq) + G(q) + F(q,dq)$$

$$d^2q = M^{-1}(q) * [\tau - V(q,dq) - G(q) - F(q,dq)]$$

Where:

τ **=** the end effector torque,

M = the symmetric joint-space inertia matrix,

V = describes *Coriolis* and *centripetal* effects [5, 6],

G = the gravity loading,

F = the end effector force.

5. THE VISUAL SYSTEM. IMPLEMENTATION AND SENSING

The variable elements derived from the visual system that participated in computing the inverse kinematics equations were Cx, Cy and the angle α made by the tire's axis (Figure 15). These parameters are required for each tire, so there is a need for 4 visual sensing systems. Furthermore, we also need the XYZ coordinates of each of the four tire holes. Once we acquire the coordinates of the 4 holes of a tire, the other variables can be easily deducted, as long as (Cx, Cy) is the center of the parallelepiped made by the holes and then translated with a constant k representing the width of the tire.

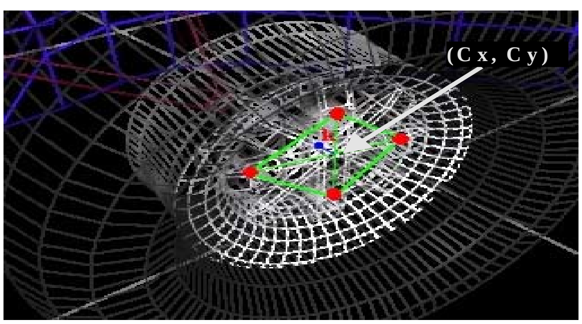

Fig. 15. Front left tire (wire-frame close-up)

The angle α represents the direction made by the 4 tire holes with the slider. ((Cx, Cy) is the center of the tire.

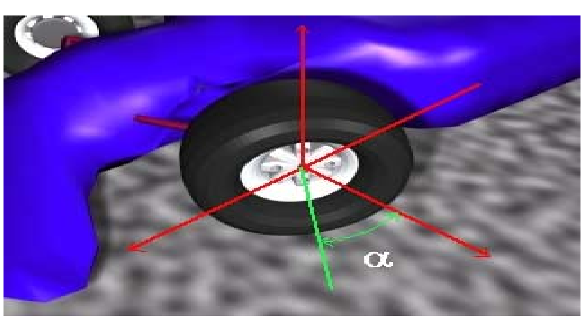

Fig. 16. Front left tire

The data that has to be supplied by the visual system consists of the tri-dimensional coordinates of 16 points (for each tire, 4 holes need to be located). The front with the rear tires will always form a same angle α, the rear tires never changing the angle relative to the rest of the car. The front tires obviously have the same axis (otherwise the car would have serious damages). The tires are always referable to each other, as long as the distance between them is constant (having a variable distance between the tires would result in abnormal situations).

Once we obtain the positions of one of the front tire's holes and one of the rear tires' holes and also their directions, we can build easily the other coordinates required. Figure 17 depicts the variable distance between the front and rear tires. If the visual system returns the orientation of the car, then this is sufficient to determine the coordinates of one of the front tires.

Fig. 17. The car (view from above)

There is also a need to control the number of times per second the visual system provides data [14]. This is important to determine the car's motion. Motion recovery would allow one arm to track the tire and to have the end - effector positioned even before the car would stop, thus gaining some time.

5.1 Technological Orientation

According to the required visual system tasks, one of possible implementations for this sensory system can be through a radio radar detector ([10, 12, 14]).

The receiving part of the system situated somewhere close to the scene will stay in stand-by mode and scan for signals from the tires. Once the receiver detects the sensors, this implies that the car is around, and according to the distance and the speed of the car the software will process and send the necessary information to the arm controller.

For the oscillations we need more frames so that the distance between the ground and tire can be analyzed. This vertical distance Δy can be calculated from two frames having holes at about the same orientation ω (please refer to the *Direct and Inverse Kinematics* section). Other tasks can be assigned to this system (i. e. analyzing the information from all the 4 tires, scanning the planarity of the car, vibrations, installation of new sensors providing different types of information, etc).

6. CONTROLING AND SUPERVISING

The following parameters will require continuous surveillance:

- engine activation requests/request-reply discrepancy, internal functionality status
- link position/orientation, requested/resulted revolution angle difference, smoothness of revolution, response time delay

- mass distribution in each arm, vibration factor evolution
- visual system supervising:
  - evolution of the delay in answering
  - discrepancy between the detected position of the holes and the one deducted from the final correction of the effector
  - internal functionality status
- tire sensors displacement in time, sensor functionality
- support displacement, internal tension during arms motions, vibration and material response
- temperature and pressure of the environment and the engines, wind velocity and direction
- parameter analysis evolution and general system status

The required joints positions and orientations are always pre-simulated and compared with the ones obtained from the direct sensor output. The parameter difference is corrected using mostly PID control. We implement digital feedback controllers for the system using a proportional plus derivative (PD) control ([7, 8,13]), simplifying considerably the nonlinear dynamic equations, but also requiring a high update rate.

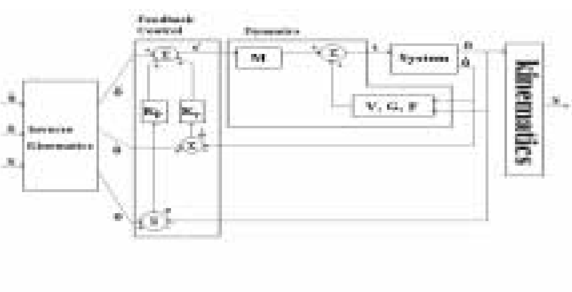

Fig. 18

6.1. Current Development Stage & Results

Currently the CAD module is connected with the kinematics and dynamics modules. Animation and simulations showing the entire tire changing process has been done too [11]. A next example (Figure 19) shows the torque applied on a joint for a *stand-by/full-extend* sequence, 1 second:

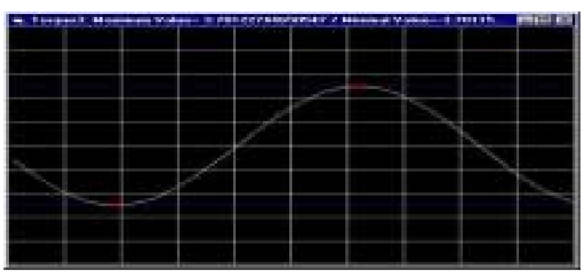

Fig. 20. Torque 3 distribution in one second.

7. CONCLUSIONS AND FUTURE WORK

The main advantage introduced by the system proposed here is the low-variance time difference (almost inexistent) for the pit stops of any team. Once a prototype is ready, further optimizations will allow minimization of this time (currently estimated at 10 seconds). A second important advantage derives from the elimination of human risks. The 5 manipulators are able not only to change the tires of a car and refuel without assistance, but to obtain critical parameters of the car and interpret it or feedback it in real-time.

Future work will address the refueling manipulator and complete the integration of the entire system within the FIA restrictions.

References

[1] Spong, W. Mark, “*Robot Dynamics and Control”*, John Wiley, 1989

[2] Dekhil, Mohamed, and Sobh, Tarek M., and Henderson, Thomas C., and Sabbavarapu, Anil, and Mecklenburg, Robert, *“Robot Manipulator Prototyping (Complete Design Review)”*, University of Utah, 1994

[3] Nakamura, Yoshihiko, *“Advanced Robotics - Redundancy and Optimization”*, Addison-Wesley, 1991

[4] Marris, Andrew W., and Stoneking, Charles E., *“Advanced Dynamics”*, McGraw-Hill, 1967

[5] Christie, Dan Edwin, *“Intermediate College Mechanics”*, McGraw-Hill, 1952

[6] De Wit, Charlos Canudas, and Siciliano, Bruno, and Bastin, Georges, *“Theory of Robot Control”*, Springer-Verlag London, 1996

[7] Sobh, Tarek M., Dekhil, Henderson, Thomas. C. and Sabbavarapu, A. “*Prototyping a Three-link Robot Manipulator,”* Sixth International Sympsium on Robotics and Manufacturing (ISRAM 96), Montpellier, France, May 1996

[8] Herrea-Beneru, L. ,Mu, E. ,Cain, J. T., “*Symbolic Computation of Robot Manipulator Kinematics*”, Department of Electrical Engineering, University of Pittsburgh

[9] Rieseler, H., Wahl, F. M., *“Fast symbolic computation of the inverse kinematics of robots*”, Institute for Robotics and computer control, Technical University of Braunschweig

[10] Dekhil, M., Sobh, T. M., Henderson, T. C. and Mecklenburg, R *“UPE: Utah Prototyping Environment for Robot Manipulators''*. In proceedings of the IEEE International Conference on Robotics and Automation, Nagoya, Japan, May 1995

[11] SCHALKOFF, R. J. *“Digital Image Processing and Computer Vision*”. John Wiley and Sons, Inc., 1989

[12] J. Hervé, P. Cucka and R. Sharma, *“Qualitative Visual Control of a Robot Manipulator''*. In Proceedings of the DARPA Image Understanding Workshop, September 1990

[13] Y. Li and W. M. Wonham, *“Controllability and Observability in the State-Feedback Control of Discrete-Event Systems''*, Proc. Conf. on Decision and Control, 1988

[14] Benedetti, R., and Risler, J.-J. *“In Real Algebraic and Semi-algebraic Sets*”, Hermann, pp. 8-19, 1990